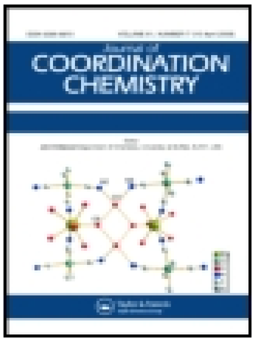

Taylor & Francis
Taylor & Francis Group

Journal of Coordination Chemistry

ISSN: 0095-8972 (Print) 1029-0389 (Online) Journal homepage: http://www.tandfonline.com/loi/gcoo20

Tetrazolate bridged dinuclear photo-luminescent zinc(II) Schiff base complex prepared via 1,3-dipolar cycloaddition at ambient condition

Satavisha Bhattacharya, Sumit Roy & Shouvik Chattopadhyay

To cite this article: Satavisha Bhattacharya, Sumit Roy & Shouvik Chattopadhyay (2016): Tetrazolate bridged dinuclear photo-luminescent zinc(II) Schiff base complex prepared via 1,3-dipolar cycloaddition at ambient condition, Journal of Coordination Chemistry, DOI: 10.1080/00958972.2016.1153078

To link to this article: http://dx.doi.org/10.1080/00958972.2016.1153078

JOURNAL OF COORDINATION CHEMISTRY, 2016
http://dx.doi.org/10.1080/00958972.2016.1153078

Taylor & Francis
Taylor & Francis Group

Tetrazolate bridged dinuclear photo-luminescent zinc(II) Schiff base complex prepared via 1,3-dipolar cycloaddition at ambient condition

Satavisha Bhattacharya, Sumit Roy and Shouvik Chattopadhyay

Department of Chemistry, Jadavpur University, Kolkata, India

ABSTRACT

A bis(μ-NN′-tetrazolate)-bridged centrosymmetric dinuclear zinc(II) Schiff base complex, $[Zn_2(L)_2(PZTZ)_2]$ (HL is a tridentate Schiff base, 2-(2-(dimethylamino) ethyliminomethyl)-6-ethoxyphenol and HPZTZ is 2-pyrazinyltetrazole), has been synthesized via [3 + 2] cycloaddition of 2-cyanopyrazine and sodium azide in the presence of zinc(II) acetate dihydrate and HL. The structure of the complex is confirmed by single-crystal X-ray diffraction analysis. The complex shows fluorescence.

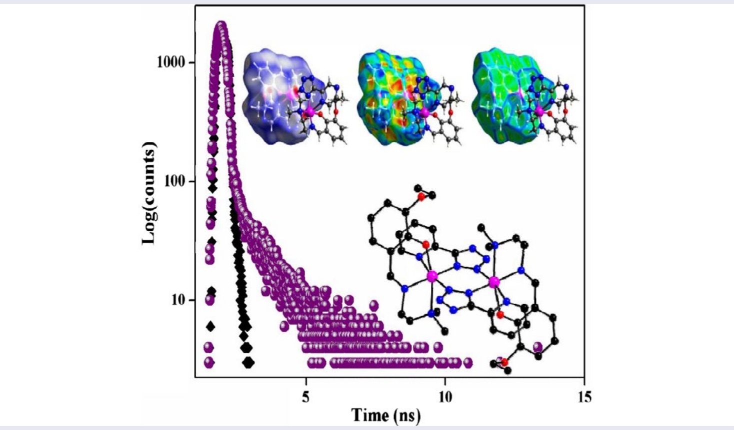

ARTICLE HISTORY
Received 1 August 2015
Accepted 29 January 2016

KEYWORDS
Zinc(II); Schiff base; 1,3-dipolar cycloaddition; 5-pyrazinyltetrazolate

1. Introduction

Di- and polynuclear zinc(II) complexes are widely used in opto-electronic devices [1, 2], catalysis [3–5], materials science [6, 7], etc. They are also used in biological modeling applications [8–10]. The ability of zinc(II) to adopt various geometries deserves further exploration of molecular architectures of new zinc(II) complexes using different bi- or polydentate chelating ligands [11–13]. Among them, tri- and tetradentate Schiff bases are the most popular for the ease of their synthesis, stability, and versatility [14–18]. Azide is also a very good co-ligand and there are many reports on the synthesis and

CONTACT Shouvik Chattopadhyay ✉ Shouvik.chem@gmail.com

characterization of various polynuclear transition and non-transition metal Schiff base complexes with azide co-ligands [14, 19–25]. These metal-ligated azides may be made to undergo 1,3-dipolar cycloaddition reactions with a suitable alkyl cyanamide to form tetrazolates which are multidentate/bridging building blocks in metal–organic frameworks [26–29]. Tetrazole functional groups are also used as a metabolically stable surrogate for a carboxylic acid group in medicinal chemistry [30], as high-density energy materials in materials science [31–33] and also as versatile ligands in coordination chemistry [34, 35]. Among a number of coordination modes of tetrazoles, the 1,2-coordination to produce bis(μ-tetrazolate)-bridged complexes is relatively common [36-38]. Zinc(II) tetrazolate-bridged complexes did not receive attention to date, possibly because of the lack of magnetic exchange interactions in them. The importance of zinc(II) complexes lies in their strong luminescence properties.

We report the tandem synthesis of a dinuclear zinc(II) Schiff base complex bridged by a substituted tetrazolate formed by reaction of 2-cyanopyrazine, sodium azide, zinc(II) acetate dihydrate, and HL {2-(2-(dimethylamino)ethyliminomethyl)-6-ethoxyphenol} under stirring in methanol. The X-ray diffraction study has confirmed the structure of the complex.

2. Experimental

All starting materials were commercially available, reagent grade, and used as-purchased from Sigma–Aldrich.

Caution!!! Azide complexes are potentially explosive. Although no problem was encountered in the present study, only small amounts of the material should be prepared and must be handled with care.

2.1. Synthesis of HL {2-(2-(dimethylamino)ethyliminomethyl)-6-ethoxyphenol}

The tetradentate N_2O_2 donor Schiff base, HL, was prepared by refluxing N,N-dimethyl-1,2-diaminoethane (1 mmol, 0.1 mL) and 3-ethoxysalicylaldehyde (1 mmol, 0.166 g) in methanol (20 mL) for *ca.* 1 h. The Schiff base was not isolated, but was used directly for preparation of the complex.

2.2. Synthesis of $[Zn_2(L)_2(PZTZ)_2]$ {bis(μ$_2$-5-(pyrazin-2-yl)tetrazolato-N,N′)-bis(2-[([2-(dimethylamino)ethyl]imino)methyl]-6-ethoxyphenolato)-di-zinc(II)}

A methanol solution of zinc(II) acetate dihydrate (1 mmol, 0.219 g) was added to methanol solution of HL, followed by addition of a methanol solution of 2-cyanopyrazine (1 mmol, 0.105 g) with stirring. A methanol solution of sodium azide (1 mmol, 0.065 g) was then added to the solution and stirred for 3 h. The resulting solution was kept at room temperature for several days to get X-ray quality yellow single crystals of the complex.

Yield: 0.20 g (55%). Anal. Calcd for $C_{36}H_{44}N_{16}O_4Zn_2$ (FW 895.65): C, 48.28; H, 4.95; N, 28.02. Found: C, 48.22; H, 4.90; N, 28.09%. IR (KBr, cm^{-1}): 1639 (C=N), 2993–2839 (CH), 1447, 1404 (tetrazole). UV–vis, λ_{max} (nm), [ε_{max} (L mol^{-1} cm^{-1})] (DMSO), 282 (5.1×10^4), 380 (2.6×10^4).

2.3. Physical measurements

Elemental analysis (carbon, hydrogen, and nitrogen) was performed on a PerkinElmer 240C elemental analyzer. The infrared spectrum, in KBr (4000–400 cm^{-1}), was recorded using a PerkinElmer Spectrum Two FTIR spectrophotometer. ESI-MS was recorded on a Qtof Micro YA263 mass spectrometer. The electronic spectrum in DMSO (800–200 nm) was recorded on a PerkinElmer Lambda 35 UV–vis spectrophotometer. The fluorescence spectrum in DMSO was obtained on a Hitachi F-7000 Fluorescence spectrophotometer at room temperature. Lifetime measurements were recorded using a Hamamatsu MCP photomultiplier (R3809) and analyzed using IBHDAS6 software.

Table 1. Crystal data and refinement details of the complex.

Formula	$C_{36}H_{44}N_{16}O_4Zn_2$
Formula weight	895.65
Temperature (K)	150
Crystal system	Monoclinic
Space group	$P2_1/n$
a (Å)	10.804(5)
b (Å)	14.690(5)
c (Å)	12.622(5)
β (°)	91.836(5)
Z	2
d_{calc} (g cm^{-3})	1.486
μ (mm^{-1})	1.259
$F(0\,0\,0)$	928
Total reflections	26,999
Unique reflections	3805
Observed data [$I > 2\sigma(I)$]	3141
No. of parameters	272
R(int)	0.035
R_1, wR_2 (all data)	0.0385, 0.0777
R_1, wR_2 [$I > 2\sigma(I)$]	0.0286, 0.0725

2.4. X-ray crystallography

X-ray single-crystal data for the complex was collected at 150 K on a Bruker APEX II diffractometer equipped with a normal focus, sealed tube X-ray source with graphite monochromated Mo-Kα radiation (λ = 0.71073 Å) operating at 50 kV and 30 mA. The programs SAINT [SMART (V 5.628), SAINT (V 6.45a), XPREP, Bruker AXS Inc., Madison, WI, 2004] were used for integration of diffraction profiles, and multi-scan empirical absorption corrections were applied to the data using SADABS [39]. The molecular structure was solved by direct methods and refined by full-matrix least squares on F^2 using the SHELX-97 package [40, 41] with anisotropic displacement parameters for all non-hydrogen atoms. Hydrogens were placed in their geometrically idealized positions and constrained to ride on their parent atoms. The crystallographic and refinement data of the complex are summarized in table 1.

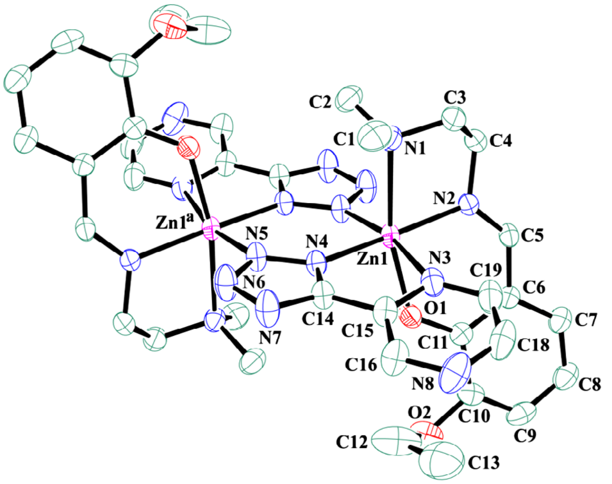

Figure 1. ORTEP view of the complex with atom numbering scheme. Thermal ellipsoids are shown at 30% probability. Hydrogens are omitted for clarity. Symmetry transformation: $^a = 1 - x, 1 - y, 1 - z$.

Table 2. Selected bond lengths (Å) of the complex.

Zn(1)–O(1)	1.9923(17)
Zn(1)–N(1)	2.373(2)
Zn(1)–N(2)	2.0233(19)
Zn(1)–N(3)	2.568(2)
Zn(1)–N(4)	2.0874(19)
$Zn(1)^a$–N(5)	2.135(2)

Note: Symmetry transformation $^a = 1 - x, 1 - y, 1 - z$.

Table 3. Selected bond angles (°) of the complex.

O(1)–Zn(1)–N(1)	165.15(16)	N(1)–Zn(1)–N(4)	91.49(6)
O(1)–Zn(1)–N(2)	91.38(6)	N(1)–Zn(1)–$N(5)^a$	94.08(7)
O(1)–Zn(1)–N(3)	80.56(6)	N(2)–Zn(1)–N(4)	163.63(7)
O(1)–Zn(1)–N(4)	95.21(6)	N(2)–Zn(1)–$N(5)^a$	98.03(7)
O(1)–Zn(1)–$N(5)^a$	98.40(6)	N(3)–Zn(1)–N(4)	71.90(6)
N(1)–Zn(1)–N(2)	78.87(7)	N(3)–Zn(1)–$N(5)^a$	167.43(6)
N(1)–Zn(1)–N(3)	88.99(6)	N(4)–Zn(1)–$N(5)^a$	95.81(6)
N(2)–Zn(1)–N(3)	94.53(6)		

Note: Symmetry transformation $^a = 1 - x, 1 - y, 1 - z$.

2.5. Hirshfeld surface analysis

Hirshfeld surfaces [42–44] and the associated 2-D fingerprint [45–47] plots were calculated using Crystal Explorer [48] with bond lengths to hydrogens set to standard values [49]. For each point on the Hirshfeld isosurface, two distances, d_e (the distance from the point to the nearest nucleus external to the surface) and d_i (the distance to the nearest nucleus internal to the surface), are defined. The normalized contact distance (d_{norm}) based on d_e and d_i is given by:

Table 4. Selected zinc(II)–$N_{pyrazinyl}$ distances (Å) in some reported complexes.

Complex	Distance (Å)	Ref.
$[Zn_2(L)_2(PZTZ)_2]$	2.568(2)	This work
$[Zn(sac)_2(\mu\text{-}pyz)(H_2O)_2]_n$	2.214(2)	[55]
$[Zn(phen)(DPZDA)(H_2O)]\cdot 2H_2O$	2.087(3)	[56]
$Zn(2,6\text{-}PZDC)(H_2O)_2$	2.049(3)	[57]
$\{[Zn(pyzn)(SCN)(H_2O)_2]\cdot H_2O\}_\infty$	2.214(2)	[58]
$(H_3O)_2[Zn(2,3PZDC)_2]$	2.184(2)	[59]
$[Zn_2(H_2O)_4(dipic)_2(\mu\text{-}apyz)]$	2.130(4), 2.065(2)	[60]
$[(Zn(DMPZ)_2Cl_2]$	2.103(1)	[61]
$1aZnCl_2$	2.217(2)	[62]
$[Zn(N_3)_2(AMPYZ)_2]$	2.037(2)	[63]
$[Zn_2(pztc)(phen)_4]\cdot 12H_2O$	2.332(3)	[64]
$[Zn_2(pz25dc)(phen)_4](NO_3)_2\cdot 10H_2O$	2.229(4)	[64]
$Zn(pyz)(NCMe)_2[AuBr_2(CN)_2]_2$	2.19(1)	[65]
$[Zn(ptp)(H_2O)]_2$	2.131(3)	[66]
$[Zn(ptp)]_n$	2.228(3)	[66]
$[Zn(pzta)_2(H_2O)_2]$	2.197(2)	[67]
$[ZnCl_2(AMPYZ)_2]$	2.058(1)	[68]
$Zn(L^1)_2(H_2O)_2$	2.213(3)	[69]
$Zn(L^2)_2(H_2O)_2$	2.185(2)	[70]
$Zn(L^3)_2(Cl)_2$	2.241(2)	[71]
$[Zn(PZTZ)_2(H_2O)_2]$	2.194(2)	[72]

Notes: HL = 2-(2-(dimethylamino)ethyliminomethyl)-6-ethoxyphenol; HPZTZ = 2-pyrazinyltetrazole; Pyz = pyrazine, and sac = saccharinate; Phen = 1,10-phenanthroline; H_2DPZDA = 3,5-dimethyl-2,6-pyrazinedicarboxylic acid; Pyzn = pyrazine-2-carboxylic anion; 2,6-PZDC = pyrazine-2,6-dicarboxylate; 2,3-PZDC = pyrazine-2,3-dicarboxylate; $dipicH_2$ = dipicolinic acid; apyz = 2-aminopyrazine; DMPZ = 2,5-dimethylpyrazine; 1a = 2-(6′,2″-bipyrid-2′-yl)-3-(2-pyridyl)pyrazine; pz25dc = pyrazine-2,5-dicarboxylate; phen = 1,10-phenanthroline; H4pztc = pyrazine-2,3,5,6-tetracarboxylic acid; H_2ptp = 2,3-bis(pyridine-2-yl)-5,6-di-1H-tetrazol-5-ylpyrazine; pzta = pyrazinyl tetrazolate; AMPYZ = 2-aminopyrazine; HL^1 = 5-(pyrazin-2-yl)-3-(pyridin-4-yl)-1H-1,2,4-triazole; HL^2 = 5-(pyrazin-2-yl)-3-(pyridin-3-yl)-1,2,4-triazolide; L^3 = 2-(1-hydrazinylideneethyl)pyrazine.

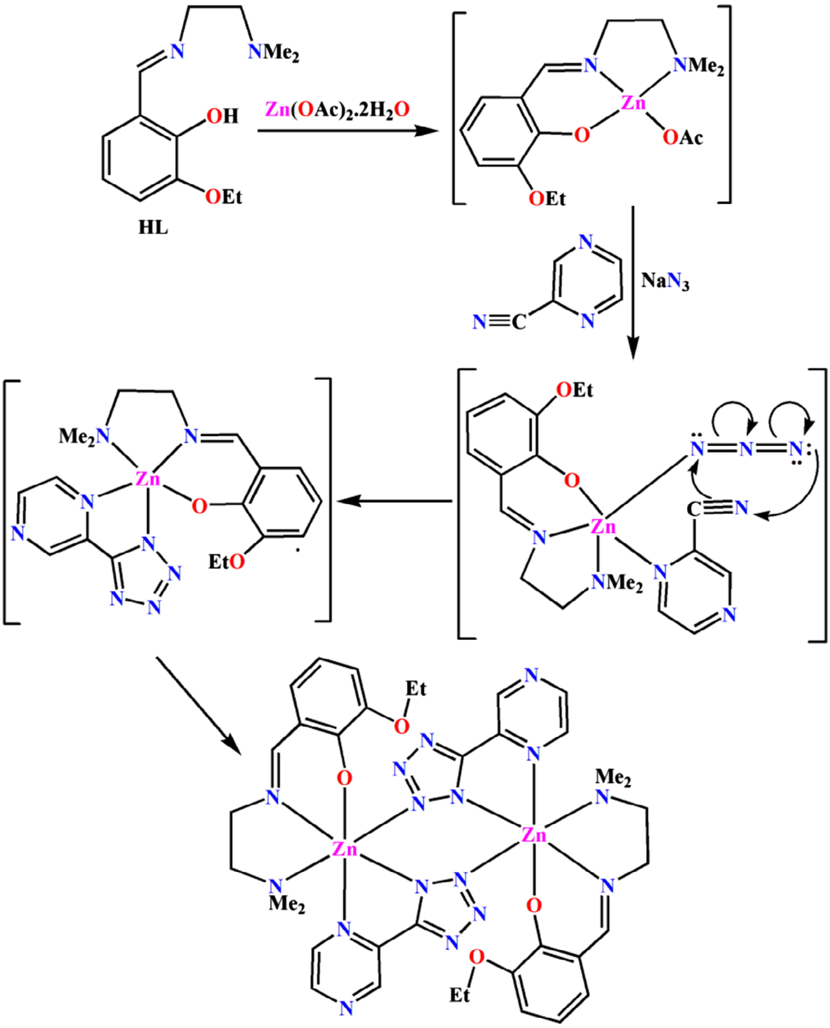

Scheme 1. The proposed route to the complex.

$$d_{\mathrm{norm}} = \frac{(d_{\mathrm{i}} - r_{\mathrm{i}}^{\mathrm{vdw}})}{r_{\mathrm{i}}^{\mathrm{vdw}}} + \frac{(d_{\mathrm{e}} - r_{\mathrm{e}}^{\mathrm{vdw}})}{r_{\mathrm{e}}^{\mathrm{vdw}}}$$

where $r_{\mathrm{i}}^{\mathrm{vdw}}$ and $r_{\mathrm{e}}^{\mathrm{vdw}}$ are the van der Waals radii of the atoms. The value of d_{norm} is negative or positive depending on intermolecular contacts being shorter or longer than the van der Waals separations. The parameter d_{norm} displays a surface with a red–white–blue color scheme, where bright red spots highlight shorter contacts, white areas represent contacts around the van der Waals separation, and blue regions are devoid of close contacts. For a given crystal structure and set of spherical atomic electron densities, the Hirshfeld surface is unique [50], and thus, it suggests the possibility of gaining additional insight into the intermolecular interactions of molecular crystals.

Table 5. Absorption and emission spectral data of some selected dizinc complexes.

Complex	$\lambda_{excitation}$	$\lambda_{emission}$	Ref.
$[Zn_2(L)_2(PZTZ)_2]$	380	432	This work
$[Zn_2(HL^1)_4](ClO_4)_4$	371	415	[54]
$[(HL^2)Zn_2(L^2)(dca)_2]ClO_4$	363	403	[54]
$[(HL^3)Zn^2(L^3)(NCS)_2]ClO_4\ CH_3OH$	365	407	[54]
$[Zn_2L^4(OAc)_2(H_2O)]$	379	469	[75]
$[Zn(L^5)(\mu_{1,1}\text{-}N_3)Zn(L)(N_3)]\cdot 1.5H_2O$	375	475	[21]
$[Zn(L^5)(\mu_{1,1}\text{-}NCO)Zn(L)(NCO)]\cdot 1.5H_2O$	375	475	[21]
$[Zn(L^5)(\mu_{1,1}\text{-}NCS)Zn(L)(NCS)(OH_2)]$	370	495	[21]
$[Zn_2(L^6)_2Cl_2]$	370	445	[16]
$[Zn_2(L^6)_2Br_2]$	370	445	[16]
$[Zn_2(L^6)_2I_2]$	370	448	[16]
$[(N_3)Zn(L^7)(\mu_{1,1}\text{-}N_3)]_2$	344	505	[76]
$[Zn_2(HL^8)_2]$	370	489	[77]
$[Zn_2(L^9)_2(\mu\text{-}tp)](ClO_4)_2$	326	370, 430	[78]
$[Zn_2(L^9)_2(\mu\text{-}tp)](PF_6)_2$	315	485	[78]
$[Zn_2L^{10}Cl_3]$	382	450	[79]
$[Zn_2L^{11}Cl_3]$	384	452	[79]
$[Zn(H)L^{12}Cl^2]\cdot H_2O$	380	481	[79]

Notes: see Table 4 for some abbreviations; HL^1 = [2-(-(3-(dimethylamino)propylimino)methyl)-4-bromophenol]; HL^2 = [2-(-(3-(dimethylamino)propylimino)methyl)-6-methoxyphenol]; HL^3 = [2-(-(3-(dimethylamino)propylimino)methyl)-6-ethoxyphenol]; H_2L^4 = N,N′-bis(salicylidene)cyclohexane-1,2-diamine; H_2L^5 = 2-(2-(dimethylamino)ethylimino)methyl)-6-methoxyphenol; H_2L^6 = 2-(2-(2-pyridyl)ethyl)imino)methyl]phenol; L^7 = N-(4,6-dimethylpyrimidin-2-yl)- N′-(1-pyridin-2-yl-ethylidine)-hydrazine; H_3L^8 = 2,6-diformyl-4-methylphenol-di(benzoylhydrazone; L^9 = N,N′-(bis(pyridin-2-yl)benzylidene)-1,3-propanediamine, tp = terephthalate dianion; HL^{10} = 2,6-bis[1-(2-aminoethyl)pyrolidine-iminomethyl]-4-methyl-phenol; HL^{11} = 2,6-bis[1-(2-aminoethyl)piperidine-iminomethyl]-4-methyl-phenol; HL^{12} = N-{1-(2-aminoethyl)pyrolidine}salicylideneimine.

3. Results and discussion

3.1. Synthesis

The potential tetradentate Schiff base (HL) was prepared by condensation of 3-ethoxysalicylaldehyde with N,N-dimethyl-1,2-diaminoethane following the literature methods [51, 52]. The ligand is not isolated and was used directly for the preparation of the complex. The methanol solution of HL was then combined with zinc(II) acetate dihydrate. Addition of 2-cyanopyrazine and sodium azide in this solution with constant stirring produced the 2-pyrazinyl tetrazolate complex of zinc(II) containing a Schiff base via [2 + 3] cycloaddition. The synthesis of the complex is shown in scheme 1.

Addition of zinc(II) is essential for synthesis in that the cyclization does not occur under ambient conditions in the absence of suitable transition metals. Use of nickel(II)/cadmium(II) produces similar

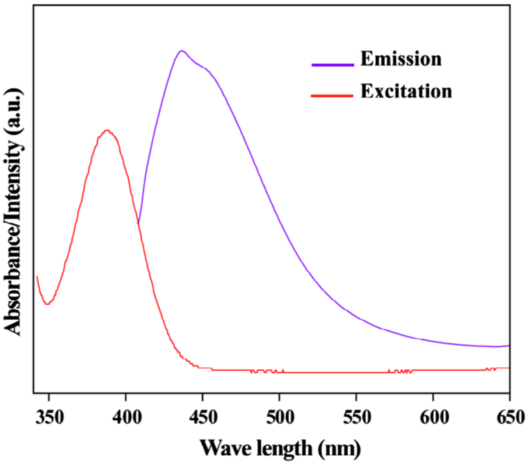

Figure 2. Excitation and emission spectra of the complex in DMSO solution.

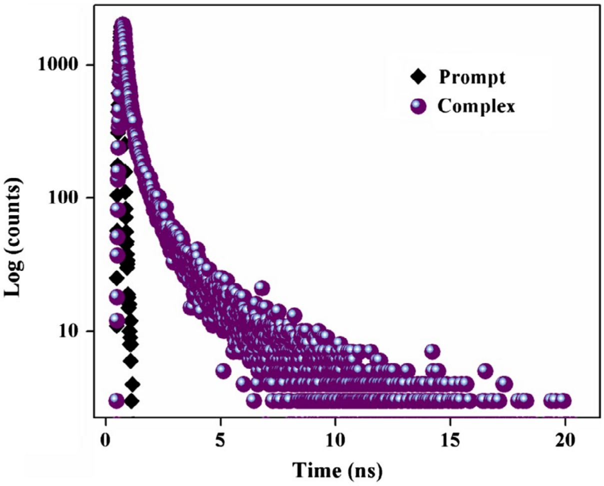

Figure 3. Lifetime decay profile of the complex.

Table 6. The detailed data of the photoluminescence and time-resolved photoluminescence decays of the complex.

λ_{ex} (nm)	λ_{em} (nm)	A_1 (%)	τ_1 (ns)	A_2 (%)	τ_2 (ns)	τ_{av} (ns)	χ^2
380	432	62.59	2.24	37.41	11.48	9.20	1.10304

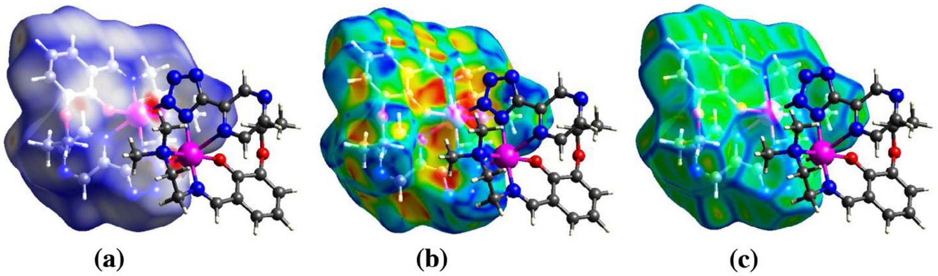

Figure 4. Hirshfeld surfaces mapped over d_{norm} (a), shape index (b), and curvedness (c) of the complex.

complexes [36, 37, 53]. However, in the absence of suitable transition metals, tetrazoles could not be isolated from the reaction mixture, as confirmed by the HRMS spectra of the reaction mixtures.

We have repeated the reaction changing the sequence of the addition of the reagents. Mass spectra of the reaction mixture do not support the formation of $[Zn_2(L)_2(PZTZ)_2]$. Thus, we conclude that the sequence of addition of different ligands is necessary for $[Zn_2(L)_2(PZTZ)_2]$ formation. The following mechanism may be proposed for formation of the complex. Three coordination sites at zinc(II) are coordinated with the tridentate Schiff base, while the fourth and fifth coordination sites are occupied by the 2-cyanopyrazine and azide. Coordination to zinc(II) makes azide a better electrophile and it undergoes a 1,3-dipolar cycloaddition with the nitrile group of 2-cyanopyrazine under ambient conditions to form the tetrazolate, which binds another zinc(II) to form $[Zn_2(L)_2(PZTZ)_2]$. The proposed mechanism is shown in scheme 1.

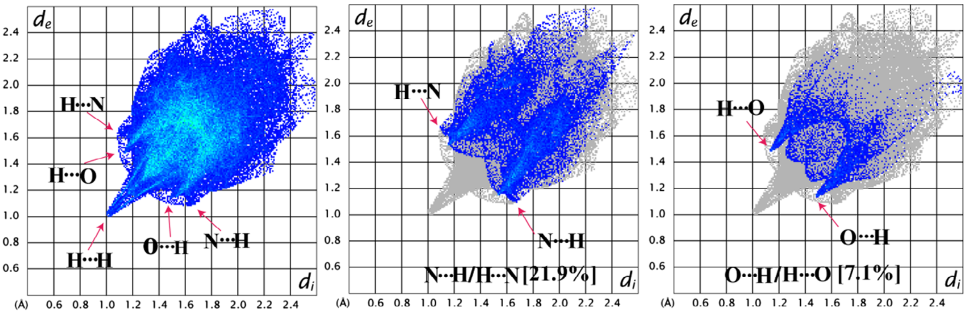

(a) (b) (c)

Figure 5. Fingerprint plots of the complex: full (a) and resolved into N···H/H···N (b) and O···H/H···O (c) contacts showing the percentages of contacts contributed to the total Hirshfeld surface area of the complex.

3.2. Description of the structure of [$Zn_2(L)_2(PZTZ)_2$]

The complex crystallizes in the monoclinic space group $P2_1/n$. The perspective view is shown in figure 1. Selected bond lengths and angles are given in tables 2 and 3, respectively. The complex features a double μ-NN′-tetrazolate-bridged zinc(II) dinuclear core, in which two distorted octahedral zinc(II) centers are bridged by two centrosymmetrically related tetrazolate ions. Within the dinuclear unit, each distorted octahedral zinc(II) center is coordinated meridionally by O(1), N(1), and N(2) of a deprotonated tridentate L^- and N(3) and N(4) of the 2-pyrazinyltetrazolate $(PZTZ)^-$. A symmetry related nitrogen, $N(5)^a$ (symmetry transformation $^a = 1-x, 1-y, 1-z$), from a bridging $(PZTZ)^-$ coordinates to complete the distorted octahedral geometry of zinc(II).

The Zn(1)–N_{imine} distance (2.0233(19) Å) is shorter than the Zn(1)–N_{amine} distance (2.373(2) Å), as observed in similar systems [54]. However, Zn(II)–$N_{pyrazinyl}$ distances (2.568(2) (Å)) for this complex are longer than distances in related zinc complexes [55–72] (table 4). The long Zn(II)–$N_{pyrazinyl}$ bond is probably a result of the bond angles with respect to chelation of the tetrazolate/pyrazine ring about zinc(II) and the bridging nature of the tetrazolate itself which prevents that portion of the ligand from "moving" to accommodate a shorter Zn(II)–$N_{pyrazinyl}$ bond length. It should be noted that the μ-NN′ bridging geometry of $(PZTZ)^-$ is asymmetric, which can be seen from the inequality in the bridging angles Zn–N(4)–N(5) = 134.2°(1) and Zn^a–N(5)–N(4) = 129.1°(1), as observed in similar complexes [38]. The saturated five-membered ring Zn–N(1)–C(3)–C(4)–N(2) assumes a half-chair conformation with puckering parameters $q(2) = 0.445(3)$ Å and $\phi(2) = 92.1(2)°$ [73]. The N(1)–Zn(1)–N(2) angle is 78.87(7)°, typical of a five-membered chelate ring [74]. There are no other significant interactions present in the complex.

3.3. IR, electronic and fluorescence spectra

Formation of a tetrazole group is further supported by the appearance of sharp bands at 1447 and 1404 cm^{-1} [37]. The IR band corresponding to the imine (C=N) stretch appears at 1639 cm^{-1} [51]. Absence of an azide peak at ~2100 cm^{-1} in the IR spectrum of the complex supports the proposed reaction between the nitrile and the azide. Bands at 2993–2839 cm^{-1} due to alkyl C–H bond stretching vibrations are in the spectrum of the complex [52]. The electronic spectrum was recorded in DMSO from 200 to 800 nm. The complex shows intense absorptions at 282 and 380 nm which may be assigned as π–π^* and n–π^* transitions, respectively [54]. The complex exhibits luminescence at 432 nm upon excitation at 380 nm, assigned as an intra-ligand (π–π^*) fluorescence. Absorption and emission spectral data of some selected dizinc complexes [16, 21, 54, 75–79] are provided in table 5 in order to have a better understanding of the photoluminescence properties of dizinc complexes. The excitation and emission spectrum of the complex is shown in figure 2. The mean lifetime of the excited state is 9.2 ns at room temperature. The decay profile (figure 3) has been fitted to a multi-exponential model:

Table 7. Hirshfeld surface analysis of some related complexes showing the percentages of contacts contributed to the total Hirshfeld surface area.

Complex	H···H (%)	N···H/H···N (%)	O···H/H···O (%)	Ref.
$[Zn_2(L)_2(PZTZ)_2]$	50.8	21.9	7.1	This work
$[Cd(PRTZ)(L^1)(OH_2)]$	50.5	17.1	6.5	[53]
$[Cd(PRTZ)(L^2)(OH_2)]$	53.9	16.5	4.9	[53]
$[Cd(PZTZ)(L^2)(OH_2)]\cdot 0.25H_2O$	48.8	18.1	11	[53]
$[Ni_2(L^3)_2(PZTZ)_2]\cdot 2(CH_3)_2SO\cdot 2.69H_2O$	49.5	14.9	13.9	[36]
$2[Ni_2(L^4)_2(PZTZ)_2]\cdot 3H_2O$	49.3	19.9	6.1	[36]
$[Ni_2(L^6)_2(PRTZ)_2]$	58.5	12.6	6	[37]
$[Ni_2(L^5)_2(PZTZ)_2]\cdot 2H_2O\cdot 2CH_3CN$	47	28.3	4	[38]
$[Ni_2(L^4)_2(PRTZ)_2Na(H_2O)]ClO_4\cdot H_2O$	37.8	8.1	18.8	[37]
$[Ni(L^3)(PRTZ)]_2$	60.4	6.2	11.8	[81]

Note: See tables 4 and 5 for abbreviations.

$$I(t) = \sum_i \alpha_i \exp\left(-t/\tau_i\right)$$

where bi-exponential functions are used to fit the emission of the complex, obtaining χ^2 close to 1. The detailed data of the photoluminescence and time-resolved photoluminescence decay of the complex are given in table 6.

3.4. *Hirshfeld surface analysis*

The Hirshfeld surfaces of the complex, mapped over d_{norm}, shape index, and curvedness are illustrated in figure 4. The surfaces are shown as transparent to allow visualization of the molecular moiety around which they are calculated. The dominant interaction between N···H and O···H atoms can be seen in the Hirshfeld surfaces as red spots on the d_{norm} surface in figure 4(a). Other visible spots in the Hirshfeld surfaces correspond to H···H contacts. The small extent of area and light color on the surface indicates weaker and longer contacts other than hydrogen bonds. The H···H, N···H, and O···H interactions appear as distinct spikes in the 2-D fingerprint plot (figure 5). Complementary regions are visible in the fingerprint plots where one molecule is a donor ($d_e < d_i$) and the other an acceptor ($d_e > d_i$). The fingerprint plots can be decomposed to highlight particular atom pair close contacts [80]. This decomposition enables separation of contributions from different interaction types, which overlap in the full fingerprint. The proportion of N···H/H···N and O···H/H···O interactions comprise 21.9 and 7.1% of the Hirshfeld surfaces for each molecule. We have compared Hirshfeld surface analysis of some related metal tetrazolate complexes with similar ligands [36–38, 53, 81] and gathered the results in table 7. The interactions also appear as two distinct spikes in the 2-D fingerprint plot (figure 5). The upper spike corresponding to the donor spike represents the H···N interactions (d_i = 1.09, d_e = 1.68 Å) and H···O interactions (d_i = 1.13, d_e = 1.48 Å). The lower spike being an acceptor spike represents the N···H interactions (d_e = 1.1, d_i = 1.7 Å) and O···H interactions (d_e = 1.12, d_i = 1.5 Å) in the fingerprint plot.

4. Conclusion

We prepared a bis(tetrazolate)-bridged dinuclear zinc(II) complex with a Schiff base as the blocking ligand under non-hydrothermal and non-microwave reaction conditions. Participation of the tetrazolate in a (μ-NN′) fashion forms a dinuclear zinc(II) complex. The facile synthesis of the complex affords a convenient synthetic route for this type of complex and opens up new possibilities for the synthesis of tetrazolate-bridged zinc(II) complexes with Schiff base co-ligands. Work is in progress to improve the yield of the reaction and to develop more systems based on this strategy to generalize the concept.

Supplementary material

Crystallographic data for the analysis have been deposited with the Cambridge Crystallographic data Center, CCDC No. 1408321. The data can be obtained free of charge from CCDC via www.ccdc.cam.ac.uk/data_request/cif.

Acknowledgment

Crystallographic data were collected at the DST-FIST, India-funded single crystal diffractometer facility at the Department of Chemistry, Jadavpur University.

Disclosure statement

No potential conflict of interest was reported by the authors.

References

[1] P.D. Vellis, J.A. Mikroyannidis, C.-N. Lo, C.-S. Hsu. *J. Polym. Sci., Part A: Polym. Chem.*, **46**, 7702 (2008).
[2] A. Winter, C. Friebe, M. Chiper, M.D. Hager, U.S. Schubert. *J. Polym. Sci.: Part A: Polym. Chem.*, **47**, 4083 (2009).
[3] M.P. Coles, P.B. Hitchcock. *Eur. J. Inorg. Chem.*, 2662 (2004).
[4] J.S. Seo, D. Whang, H. Lee, S.I. Jun, J. Oh, Y.J. Jeon, K. Kim. *Nature*, **404**, 982 (2000).
[5] M. Zulkefeli, A. Suzuki, M. Shiro, Y. Hisamatsu, E. Kimura, S. Aoki. *Inorg. Chem.*, **50**, 10113 (2011).
[6] M. Döring, M. Ciesielski, O. Walter, H. Görls. *Eur. J. Inorg. Chem.*, 1615 (2002).
[7] X. Wang, C. Qin, E. Wang, Y. Li, N. Hao, C. Hu, L. Xu. *Inorg. Chem.*, **43**, 1850 (2004).
[8] J.A. Drewry, P.T. Gunning. *Coord. Chem. Rev.*, **255**, 459 (2011).
[9] F. Mancin, P. Tecilla. *New J. Chem.*, **31**, 800 (2007).
[10] A. Erxleben, J. Hermann. *J. Chem. Soc., Dalton Trans.*, 569 (2000).
[11] M. Eddaoudi, D.B. Moler, H. Li, B. Chen, T.M. Reineke, M. O'Keeffe, O.M. Yaghi. *Acc. Chem. Res.*, **34**, 319 (2001).
[12] G.-X. Liu, Y.-Q. Huang, Q. Chu, T. Okamura, W.-Y. Sun, H. Liang, N. Ueyama. *Cryst. Growth Des.*, **8**, 3233 (2008).
[13] Q.-G. Zhai, X.-Y. Wu, S.-M. Chen, C.-Z. Lu, W.-B. Yang. *Cryst. Growth Des.*, **6**, 2126 (2006).
[14] Y. Yue, E. Gao, C. Fang, T. Zheng, J. Liang, C.H. Yan. *CrystEngComm*, **10**, 614 (2008).
[15] S. Sen, P. Talukder, S.K. Dey, S. Mitra, G. Rosair, D.L. Hughes, G.P.A. Yap, G. Pilet, V. Gramlich, T. Matsushita. *Dalton Trans.*, 1758 (2006).
[16] P. Chakraborty, A. Guha, S. Das, E. Zangrando, D. Das. *Polyhedron*, **49**, 12 (2013).
[17] W.L. Tong, S.M. Yiu, M.C.W. Chan. *Inorg. Chem.*, **52**, 7114 (2013).
[18] G. Consiglio, S. Failla, P. Finocchiaro, I.P. Oliveri, S.D. Di Bella. *Inorg. Chem.*, **51**, 8409 (2012).
[19] Z.-L. You, P. Hou, L.-L. Ni, S. Chen. *Inorg. Chem. Commun.*, **12**, 444 (2009).
[20] R.-H. Hui, P. Zhou, Z.-L. You. *Synth. React. Inorg. Met.-Org. Nano-Met. Chem.*, **42**, 135 (2012).
[21] S. Basak, S. Sen, S. Banerjee, S. Mitra, G. Rosair, M.T.G. Rodriguez. *Polyhedron*, **26**, 5104 (2007).
[22] Q. Wang. *Acta Cryst.*, **E62**, m2043 (2006).
[23] M. Sarkar, R. Clérac, C. Mathonière, N.G.R. Hearns, V. Bertolasi, D. Ray. *Inorg. Chem.*, **50**, 3922 (2011).
[24] Y. Song, C. Massera, O. Roubeau, P. Gamez, A.M.M. Lanfredi. *Inorg. Chem.*, **43**, 6842 (2004).
[25] S. Mukherjee, P.S. Mukherjee. *Dalton Trans.*, **42**, 4019 (2013).
[26] S. Jeong, X. Song, S. Jeong, M. Oh, X. Liu, D. Kim, D. Moon, M.S. Lah. *Inorg. Chem.*, **50**, 12133 (2011).
[27] K. Darling, W. Ouellette, A. Prosvirin, S. Walter, K.R. Dunbar, J. Zubieta. *Polyhedron*, **58**, 18 (2013).
[28] D.-X. Xue, A.J. Cairns, Y. Belmabkhout, L. Wojtas, Y. Liu, M.H. Alkordi, M. Eddaoudi. *J. Am. Chem. Soc.*, **135**, 7660 (2013).
[29] J.-Y. Sun, L. Wang, D.-J. Zhang, D. Li, Y. Cao, L.-Y. Zhang, S.-L. Zeng, G.-S. Pang, Y. Fan, J.-N. Xu, T.-Y. Song. *CrystEngComm*, **15**, 3402 (2013).
[30] H. Singh, A.S. Singh Chawla, V.K. Kapoor, D. Paul, R.K. Malhotra. *Prog. Med. Chem.*, **17**, 151 (1980).
[31] V.A. Ostrovskii, M.S. Pevzner, T.P. Kofmna, M.B. Shcherbinin, I.V. Tselinskii. *Targets Heterocycl. Syst.*, **3**, 467 (1999).
[32] M. Hiskey, D.E. Chavez, D.L. Naud, S.F. Son, H.L. Berghout, C.A. Bome. *Proc. Int. Pyrotech. Semin.*, **27**, 3 (2000).
[33] Q. Wu, W. Zhu, H. Xiao. *J. Chem. Eng. Data*, **58**, 2748 (2013).
[34] H. Zhao, Z.-R. Qu, H.-Y. Ye, R.-G. Xiong. *Chem. Soc. Rev.*, **37**, 84 (2008).
[35] Z. Li, M. Li, X.-P. Zhou, T. Wu, D. Li, S.W. Ng. *Cryst. Growth Des.*, **7**, 1992 (2007).
[36] M. Das, K. Harms, B.N. Ghosh, K. Rissanen, S. Chattopadhyay. *Polyhedron*, **87**, 286 (2015).
[37] M. Das, S. Chatterjee, K. Harms, T.K. Mondal, S. Chattopadhyay. *Dalton Trans.*, **43**, 2936 (2014).
[38] M. Das, K. Harms, S. Chattopadhyay. *Dalton Trans.*, **43**, 5643 (2014).
[39] G.M. Sheldrick, *SADABS: Software for Empirical Absorption Correction*, University of Gottingen, Institute fur Anorganische Chemieder Universitat, Gottingen, Germany (1999–2003).
[40] G.M. Sheldrick. *Acta Cryst.*, **64**, 112 (2008).

[41] G.M. Sheldrick. *SHELXS-97 and SHELXL-97: Program for Structure Solution*, University of Göttingen, Institute fur Anorganische Chemieder Universitat, Gottingen, Germany (1997).

[42] M.A. Spackman, D. Jayatilaka. *CrystEngComm*, **11**, 19 (2009).

[43] F.L. Hirshfeld. *Theor. Chim. Acta*, **44**, 129 (1977).

[44] H.F. Clausen, M.S. Chevallier, M.A. Spackman, B.B. Iversen. *New J. Chem.*, **34**, 193 (2010).

[45] A.L. Rohl, M. Moret, W. Kaminsky, K. Claborn, J.J. McKinnon, B. Kahr. *Cryst. Growth Des.*, **8**, 4517 (2008).

[46] A. Parkin, G. Barr, W. Dong, C.J. Gilmore, D. Jayatilaka, J.J. McKinnon, M.A. Spackman, C.C. Wilson. *CrystEngComm*, **9**, 648 (2007).

[47] M.A. Spackman, J.J. McKinnon. *CrystEngComm*, **4**, 378 (2002).

[48] S.K. Wolff, D.J. Grimwood, J.J. McKinnon, D. Jayatilaka, M.A. Spackman, *Crystal Explorer 2.0*, University of Western Australia, Perth, Australia (2007). Available online at: http://hirshfeldsurfacenet.blogspot.com/.

[49] F.H. Allen, O. Kennard, D.G. Watson, L. Brammer, A.G. Orpen, R.J. Taylor. *J. Chem. Soc., Perkin Trans.*, **2**, S1 (1987).

[50] J.J. Kinnon, M.A. Spackman, A.S. Mitchell. *Acta Cryst.*, **B60**, 627 (2004).

[51] S. Roy, S. Chattopadhyay. *Inorg. Chim. Acta*, **433**, 72 (2015).

[52] S. Roy, K. Harms, S. Chattopadhyay. *Polyhedron*, **91**, 10 (2015).

[53] P.K. Bhaumik, S. Roy, K. Harms, S. Chattopadhyay. *Polyhedron*, **81**, 168 (2014).

[54] A. Bhattacharyya, S. Sen, K. Harms, S. Chattopadhyay. *Polyhedron*, **88**, 156 (2015).

[55] V.T. Yilmaz, E. Senel, C. Kazak. *J. Coord. Chem.*, **61**, 2675 (2008).

[56] Y.-G. Sun, X.-F. Gu, R. Drozdzak, F. Ding, E.-J. Gao, X.-M. Yan, F. Verpoort. *J. Coord. Chem.*, **61**, 1839 (2008).

[57] M. Gryz, W. Starosta, H. Ptasiewicz-Bąk, J. Leciejewicz. *J. Coord. Chem.*, **56**, 1575 (2003).

[58] J.-M. Li, J.-M. Shi, C. Wu, W. Xu. *J. Coord. Chem.*, **56**, 869 (2003).

[59] M. Gryz, W. Starosta, J. Leciejewicz. *J. Coord. Chem.*, **58**, 931 (2005).

[60] M. Tabatabaee, S. Rashidi, M. Islaminia, M. Ghassemzadeh, K. Molčanov, B. Neumüller. *J. Coord. Chem.*, **65**, 3449 (2012).

[61] M. Wriedt, I. Jeß, C. Näther. *Eur. J. Inorg. Chem.*, 363 (2009).

[62] S.I.G. Dias, F. Heirtzler, T. Bark, G. Labat, A. Neels. *Polyhedron*, **23**, 1011 (2004).

[63] M.A.S. Goher, F.A. Mautner, B. Sodin, B. Bitschnau. *J. Mol. Struct.*, **96**, 879 (2008).

[64] A.-H. Yang, Y.-P. Quan, H.-L. Gao, S.-R. Fang, Y.-P. Zhang, L.-H. Zhao, J.-Z. Cui, J.-H. Wang, W. Shi, P. Cheng. *CrystEngComm*, **11**, 2719 (2009).

[65] J.S. Ovens, D.B. Leznoff. *Dalton Trans.*, **40**, 4140 (2011).

[66] T.-L. Hu, Y. Tao, Z. Chang, X.-H. Bu. *Inorg. Chem.*, **50**, 10994 (2011).

[67] Z. Li, M. Li, X.-P. Zhou, T. Wu, D. Li, S.W. Ng. *Cryst. Growth Des.*, **7**, 1992 (2007).

[68] S. Gao, S.W. Ng. *Acta Cryst.*, **E67**, m1049 (2011).

[69] B. Li, P.-W. Liu, J. Chen. *Acta Cryst.*, **E68**, m203 (2012).

[70] Y.-N. Wang, W.-W. Dong. *Acta Cryst.*, **E70**, m116 (2014).

[71] L.-L. Liang, M. Li, J.-C. Liu, Y. Wei. *Acta Cryst.*, **E68**, m710 (2012).

[72] J. Luo, X.-R. Zhang, L.-L. Cui, W.-Q. Dai, B.-S. Liu. *Acta Cryst.*, **C62**, m614 (2006).

[73] D. Cremer, J.A. Pople. *J. Am. Chem. Soc.*, **97**, 1354 (1975).

[74] P. Kundu, P. Chakraborty, J. Adhikary, T. Chattopadhyay, R.C. Fischer, F.A. Mautner, D. Das. *Polyhedron*, **85**, 320 (2015).

[75] Y. Zhang, W. Feng, H. Liu, Z. Zhang, X. Lü, J. Song, D. Fan, W.-K. Wong, R.A. Jones. *Inorg. Chem. Commun.*, **24**, 148 (2012).

[76] S. Ray, S. Konar, A. Jana, S. Jana, A. Patra, S. Chatterjee, J.A. Golen, A.L. Rheingold, S.S. Mandal, S.K. Kar. *Polyhedron*, **33**, 82 (2012).

[77] K. Das, T.K. Mondal, E. Garribba, M. Fondo, C. Sinha, A. Datta. *Inorg. Chim. Acta*, **413**, 194 (2014).

[78] S. Roy, B.N. Sarkar, K. Bhar, S. Satapathi, P. Mitra, B.K. Ghosh. *J. Mol. Struct.*, **1037**, 160 (2013).

[79] T. Chattopadhyay, M. Mukherjee, K.S. Banu, A. Banerjee, E. Suresh, E. Zangrando, D. Das. *J. Coord. Chem.*, **62**, 967 (2009).

[80] M.A. Spackman, P.G. Byrom. *Chem. Phys. Lett.*, **267**, 215 (1997).

[81] B.G. Mukhopadhyay, S. Mukhopadhyay, M.F.C. Guedes da Silva, M.A.J. Charmier, A.J.L. Pombeiro. *Dalton Trans.*, 4778 (2009).